BMC Women's Health

RESEARCH

Open Access

Identifying key palmitoylation-associated genes in endometriosis through genomic data analysis

Jinyan Kai[1], Jiaqi Su[1], Yinping You[2], Xiaoliang Liang[1], Haitao Huang[3], Jie Fang[4*] and Qiong Chen[5*]

Abstract

Background Palmitoylation, a post-translational lipid modification, has garnered increasing attention for its role in inflammatory processes and tumorigenesis. Emerging evidence suggests a potential association between palmitoylation and inflammatory responses in the pathogenesis of endometriosis. However, the precise mechanistic interplay remains elusive, necessitating further investigation.

Methods This study integrated transcriptomic analysis and Mendelian randomization (MR) to identify a causal gene set implicated in endometriosis. Differentially expressed genes (DEGs) were first identified in the training dataset using the limma package in R. Weighted gene co-expression network analysis (WGCNA) was subsequently performed, leveraging Single Sample Gene Set Enrichment Analysis (ssGSEA)-derived scores of palmitoylation-related genes (PRGs) as phenotypic traits to identify key modular genes. The intersection of these key modular genes with DEGs yielded a refined gene set. Machine learning algorithms were then applied to further optimize gene selection, followed by external validation, immune infiltration analysis, RNA network construction, and exploration of potential targeted drug candidates.

Results Through a rigorous screening process, VRK1, GALNT12, and RMI1 emerged as key genes associated with palmitoylation, exhibiting significant downregulation in endometriosis samples ($P < 0.05$), indicative of a potential protective role. Immune infiltration analysis further revealed strong correlations between these genes and M2 macrophages as well as resting Natural Killer (NK) cells. Additionally, investigations into the targeted RNA network and drug association profiling provided novel insights, laying the groundwork for future high-quality validation studies.

Conclusions This study employed a comprehensive analytical framework to identify palmitoylation-associated key genes in endometriosis. The integration of immunoinfiltration analysis, RNA network construction, and drug association profiling offers valuable insights for advancing clinical diagnostics, disease monitoring, and therapeutic development in endometriosis.

Keywords Palmitoylation, Endometriosis, Transcriptomics, Mendelian Randomization

*Correspondence:
Jie Fang
fang_jie0831@163.com
Qiong Chen
chenqiongjone@shsmu.edu.cn
Full list of author information is available at the end of the article

Introduction

Endometriosis is an estrogen-dependent chronic inflammatory condition characterized by the ectopic proliferation of endometrial-like tissue [1, 2]. Despite its histologically benign classification, the condition exhibits invasive, metastatic, and recurrent behaviors reminiscent of malignancies, affecting approximately 10% of women of reproductive age [3, 4]. Common clinical manifestations, including chronic pelvic pain, dysmenorrhea, dysuria, and infertility, substantially diminish patients' quality of life [4]. As the pathophysiology of the disease becomes increasingly understood, attention has shifted toward the roles of hormonal dysregulation, inflammatory mediators, and genetic susceptibility [5, 6]. However, definitive conclusions regarding their precise contributions remain elusive. Current therapeutic strategies primarily rely on hormonal suppression therapy and minimally invasive surgical interventions [7]. Nevertheless, these approaches are often associated with high recurrence rates and treatment-related complications [8, 9]. Given these limitations, elucidating the underlying molecular mechanisms and identifying reliable diagnostic and prognostic biomarkers represent crucial avenues for advancing precision medicine, optimizing clinical management, and mitigating disease recurrence.

Protein palmitoylation, a reversible post-translational lipid modification, is dynamically regulated by a cohort of palmitoyl S-acyltransferases characterized by the Asp-His-His-Cys (DHHC) motif [10, 11]. This process is counterbalanced by acylprotein thioesterases, which modulate protein localization and function in a highly dynamic manner [10, 11]. Recent studies have highlighted the intricate role of palmitoylation in inflammatory regulation, with ZDHHC12 promoting the degradation of NOD-like receptor family pyrin domain-containing 3 (NLRP3) through chaperone-mediated autophagy [12]. In autoinflammatory disorders, the NOD2 variant NOD2 s-R444 C demonstrates an increased affinity for ZDHHC5, leading to excessive palmitoylation and exacerbated inflammatory responses [13]. Inflammation is recognized as a central etiological factor in endometriosis. Recent findings suggest that NLRP3-mediated pyroptosis contributes to the pathogenesis of inflammatory endometriosis by driving ectopic endometrial cell proliferation and angiogenesis [14]. Targeted anti-inflammatory interventions, such as long-acting anti-IL8 antibody administration, have shown promise in mitigating disease progression [15]. Despite extensive research on palmitoylation across various biological processes [16–18], its specific role in endometriosis remains largely unexplored. Notably, ZDHHC12 has been implicated in modulating NLRP3 palmitoylation, thereby influencing its activation status and regulating myocardial inflammation, oxidative stress, and associated cellular damage [19]. Furthermore, loss of palmitoyl protein thioesterase 1 (Ppt1) impairs depalmitoylation, leading to aberrant synaptic protein trafficking and neuroinflammation through mechanisms involving A-kinase anchor protein 5 (Akap5) and nuclear factor of activated T cells (NFAT) [20]. Building on these insights, this study aims to elucidate the regulatory role of palmitoylation in the pathogenesis of endometriosis, assessing its potential as a critical modulatory mechanism. By uncovering previously unrecognized pathogenic pathways and identifying novel therapeutic targets, these findings are anticipated to advance the development of more effective treatment strategies.

By integrating transcriptomic and genomic data from the Gene Expression Omnibus (GEO) and Genome-Wide Association Studies (GWAS) databases, key palmitoylation-associated genes in endometriosis were identified through differential expression analysis, Mendelian randomization (MR), machine learning, and expression validation. Further exploration of the interplay between palmitoylation and endometriosis was conducted via immune infiltration analysis, chromosomal localization, and regulatory network reconstruction, providing a theoretical foundation for the precise diagnosis, surveillance, and therapeutic intervention of endometriosis.

Materials and methods

Data collection and extraction

Endometriosis-related datasets (GSE51981 and GSE25628) were obtained from the GEO database for transcriptomic analysis. The GSE51981 dataset, designated as the training set, comprised 77 pelvic endometriosis (PE) samples and 34 control samples, with genomic profiling conducted on the GPL570 platform. To enhance data specificity, 37 samples with uterine or pelvic pathology were excluded from the analysis. The GSE25628 dataset, serving as the independent validation set, included 16 endometriosis and 6 control endometrial tissue samples, sequenced on the GPL571 platform. Additionally, Mendelian randomization (MR) data on endometriosis were retrieved from the publicly available Integrative Epidemiology Unit (IEU) Open GWAS database. The selected dataset (ukb-b- 9668) comprised genomic data from 463,010 European individuals, including 1,121 cases and 461,889 controls, encompassing a total of 9,851,867 single nucleotide polymorphisms (SNPs). A curated list of 23 palmitoylation-related genes (PRGs) was extracted from relevant literature [21].

PRGs score and weighted gene co-expression network analysis

In the GSE51981 dataset, PRG scores were computed using single-sample gene set enrichment analysis

(ssGSEA) from the GSVA package (v1.46.0; data of use: 2024.11.20) [22], based on the differential expression of PRGs in PE and control samples. Statistical comparisons of PRG scores between PE and control groups were performed using the Wilcoxon test, with significance set at $P < 0.05$.

Weighted gene co-expression network analysis (WGCNA) was subsequently applied to identify key module genes in GSE51981, utilizing ssGSEA-derived PRG scores as trait variables via the WGCNA package (v1.7.1; data of use: 2024.11.20) [23]. Initial sample clustering was conducted to detect and eliminate outliers. The optimal soft threshold power was determined by achieving an R^2 exceeding 0.8 while maintaining near-zero mean connectivity. A co-expression matrix was then constructed using the selected soft threshold, with a minimum module size of 30 genes, a dynamic tree cut parameter of 2, and a module merging threshold of 0.25. Distinct gene modules were assigned unique color labels. Correlation coefficients between endometriosis samples, control samples, and PRG scores were computed for each module, and the associations were visualized in a heatmap. Modules demonstrating a significant correlation with PRG scores ($|r| > 0.5$, $P < 0.05$) were designated as key modules, with their constituent genes identified as key module genes.

Differential expression analysis

Differentially expressed genes (DEGs) between PE and control samples in GSE51981 were identified using the limma package (v3.54.0; data of use: 2024.11.20) [24], applying selection criteria of $|\log_2$ fold change (FC)$| > 1$ and $P < 0.05$. The distribution of DEGs was illustrated via a volcano plot and heatmap, generated using the ggplot2 package (v3.4.3; data of use: 2024.11.20) [25] and ComplexHeatmap package (v2.14.0; data of use: 2024.11.20) [26], respectively.

Function analysis

The intersecting genes were identified by overlapping DEGs with key module genes. To elucidate their functional significance, Gene Ontology (GO) and Kyoto Encyclopedia of Genes and Genomes (KEGG) pathway enrichment analyses were performed using the clusterProfiler package (v4.7.1.003; data of use: 2024.11.21) [27], with a significance threshold of $P < 0.05$. GO enrichment analysis categorized functional annotations into biological processes (BP), cellular components (CC), and molecular functions (MF).

MR study

Based on these intersecting genes, an MR analysis was conducted using the TwoSampleMR package (v0.5.6; data of use: 2024.11.21) [28], treating these genes as exposure factors and endometriosis as the outcome variable. Stringent adherence to classical MR assumptions was maintained throughout the analysis: (i) the independence assumption ensured that instrumental variables (IVs) were not confounded by external factors, (ii) the association assumption confirmed a direct influence of IVs on the exposure, and (iii) the exclusivity assumption verified that IVs affected the outcome solely through the exposure, without alternative causal pathways.

GWAS data for the intersecting genes (expression Quantitative Trait Loci, eQTL) and endometriosis (ukb-b- 9668) were retrieved from the IEU Open GWAS database. Initial IV screening was performed using the VariantAnnotation (v1.44.0; data of use: 2024.11.21) [29] and ieugwasr (v1.0.1; data of use: 2024.11.21) [30] packages, with a significance threshold of $P < 5 \times 10^{-6}$. Linkage disequilibrium (LD) filtering was applied (clump = TRUE, $R^2 = 0.001$, kb = 10), and genes with at least three SNPs (nSNP ≥ 3) were retained, ensuring harmonization of effect alleles and effect sizes. Weak IVs were identified based on the F-statistic, with IVs excluded when $F < 10$. MR analysis was conducted using five complementary methods: MR Egger [31], Weighted Median [32], Inverse Variance Weighted (IVW) [33], Simple Mode [34], and Weighted Mode [35], with IVW serving as the primary statistical approach ($P < 0.05$). Results were visualized through scatter plots, forest plots, and funnel plots. To assess the robustness of the MR findings, sensitivity analyses were performed, including heterogeneity testing (Cochran's Q test, $P > 0.05$), horizontal pleiotropy evaluation ($P > 0.05$), and leave-one-out (LOO) analysis using the mr heterogeneity [36], mr pleiotropy test [37], and mr leaveoneout [38] functions, respectively. The causal direction was further validated using the Steiger test, with a correct causal direction indicated by Steiger $P < 0.05$. Following these analyses, genes demonstrating significant causal relationships with endometriosis were identified as candidate genes for further investigation.

Machine learning and gene expression analysis

To further refine the selection of feature genes, four machine learning algorithms—Random Forest (RF), Support Vector Machine (SVM), Generalized Linear Model (GLM), and k-Nearest Neighbor (KNN)—were employed to construct predictive models based on the expression profiles of candidate genes in the GSE51981 dataset. The core reason for selecting these machine learning methods was that their advantages complemented each other, providing more comprehensive and accurate feature gene selection results. Each method had its strengths in data processing, feature importance evaluation, high-dimensional data handling, and

model interpretability. Therefore, using multiple methods for comparison improved the reliability and accuracy of the results. Model training and validation were conducted using the caret package (v6.0–93; data of use: 2024.11.21) [39]. To evaluate model performance, receiver operating characteristic (ROC) curves and residual box plots were generated using the DALEX package (v1.1.0; data of use: 2024.11.21) [40]. Additionally, gene importance scores derived from each machine learning model were visualized using bar plots. The top 10 most important genes from each model were intersected to identify a refined set of feature genes.

Expression validation of the identified feature genes was subsequently performed in both the GSE51981 and GSE25628 datasets. Wilcoxon tests were applied to compare gene expression between endometriosis and control samples, with significance set at $P < 0.05$. Genes exhibiting significant differential expression in both datasets, with a consistent expression trend, were designated as key genes.

Immune infiltration analysis

To assess immune cell infiltration in endometriosis and control samples from GSE51981, the CIBERSORT algorithm (v1.0.3; data of use: 2024.11.22) [41] was applied to estimate immune scores for 22 immune cell types. Samples with $P > 0.05$ were excluded to ensure reliable deconvolution results. Wilcoxon tests were then used to compare immune cell composition between endometriosis and control samples, and immune cell types exhibiting significant differential infiltration ($P < 0.05$) were selected for further analysis.

Spearman correlation analysis was subsequently conducted to explore relationships among the 22 immune cell types and to assess associations between key genes and differentially infiltrated immune cells, with correlation thresholds set at $|r| > 0.3$ and $P < 0.05$.

Chromosomal localization and functional similarity analyses

To determine the genomic distribution of key genes across the 23 pairs of human chromosomes, the University of California Santa Cruz (UCSC) Genome Browser (http://genome.ucsc.edu/) was utilized to retrieve their chromosomal start and stop positions. The RCircos package (v1.2.2; data of use: 2024.11.22) [42] was then employed to generate a genome-wide visualization of key gene loci. Additionally, functional relationships among the key genes were further explored using the GoSemSim package (v6.5–0; data of use: 2024.11.22) [43].

Regulation network analysis

The miRwalk (http://mirwalk.umm.uni-heidelberg.de/) and miRDB (https://mirdb.org/) databases were utilized to predict MicroRNAs (miRNAs) targeting the identified key genes. The intersection of miRNAs derived from both databases was considered the final set of key miRNAs. An mRNA-miRNA regulatory network was subsequently constructed and visualized using Cytoscape (v3.10.2; data of use: 2024.11.22) [44].

Similarly, transcription factors (TFs) associated with key genes were predicted using the hTFtarget (https://guolab.wchscu.cn/hTFtarget/#!/) and miRNet (https://www.mirnet.ca/) databases. Key TFs were identified by overlapping the predictions from both sources, and an mRNA-TF regulatory network was constructed and visualized in Cytoscape.

To further explore potential therapeutic targets, drug-gene interactions were analyzed using the Comparative Toxicogenomics Database (CTD) (http://ctdbase.org/) and the Enrichr database (https://maayanlab.cloud/Enrichr/). Drugs targeting endometriosis-associated key genes were extracted from both databases, with duplicate entries removed. An mRNA-drug interaction network was then established and visualized in Cytoscape.

Immunohistochemistry

For experimental validation, three paraffin-embedded sections of ectopic endometrial and normal endometrial tissue were collected from the Pathology Department of Shanghai General Hospital. Immunohistochemistry (IHC) was performed using primary antibodies against GALNT12 (Solarbio, K108365P, 1:100), VRK1 (Proteintech, 28,018–1-AP, 1:100), and RMI1 (Proteintech, 14630–1-AP, 1:100), diluted in Phosphate-Buffered Saline (PBS). Five-micrometer-thick paraffin sections were deparaffinized and rehydrated, followed by incubation with 0.3% H_2O_2 in methanol to inhibit endogenous peroxidase activity. After antigen retrieval and cooling, sections were blocked with 1% Bovine Serum Albumin (BSA) and incubated with primary antibodies overnight at 4 °C. The following day, sections were treated with HRP-conjugated secondary antibodies (Shanghai Long Island Biotech, Shanghai, China) for 1 h at room temperature, followed by diaminobenzidine (DAB) staining and hematoxylin counterstaining. Slides were examined and imaged under a Leica SP5 light microscope (Leica, China) at 100 × and 200 × magnification.

Statistical analysis

Statistical analyses were conducted using R (v4.2.2), with inter-group differences assessed via the Wilcoxon

test ($P < 0.05$). Regulatory networks were generated and visualized using Cytoscape (v3.10.2).

Results

Screening of palmitoacylation related gene modules in endometriosis

PRG score analysis in the GSE51981 dataset revealed significantly elevated scores in PE samples compared to controls (Fig. 1A). To further explore gene co-expression patterns, WGCNA was performed on the GSE51981 dataset. Clustering analysis confirmed the absence of outlier samples (Fig. 1B). An optimal soft-thresholding power of 19 was determined based on scale-free topology criteria ($R^2 = 0.8$) while maintaining mean connectivity near zero (Fig. 1C). Subsequently, a co-expression matrix was constructed, identifying 18 distinct modules, each represented by a unique color, with the Grey module excluded as it contained unassigned genes (Fig. 1D). Pearson correlation analysis revealed significant associations between PRG scores and two key modules: MEgreenyellow ($r = 0.68$, $P < 0.001$) and MEbrown ($r = -0.55$, $P < 0.001$) (Fig. 1E). These modules were designated as key modules, collectively encompassing 307 genes, referred to as key module genes.

Identification and functional exploration of the intersection genes

Differential expression analysis in the GSE51981 dataset identified 3,376 DEGs between endometriosis and control samples, with 1,267 genes exhibiting upregulation and 2,109 showing downregulation (Fig. 2A and B). By intersecting the 3,376 DEGs with the 307 key module genes, 204 intersection genes were identified (Fig. 2C). Functional enrichment analysis of these 204 genes revealed significant enrichment in 368 GO terms and 31 KEGG pathways. GO enrichment analysis, categorized into BP, CC, and MF, identified key terms such as"nuclear division,""chromosomal region,"and"tubulin binding"(Fig. 2D). KEGG pathway enrichment analysis highlighted pathways including"cell cycle,""mineral absorption,"and"progesterone-mediated oocyte maturation"(Fig. 2E).

Candidate genes with a significant causal relationship with endometriosis

The causal association between the 204 intersecting genes and endometriosis was further examined. Following the IV screening, 126 genes remained as exposure factors for further investigation. The MR analysis identified 17 genes with a statistically significant causal relationship with endometriosis ($P < 0.05$) (Table 1). Among them, seven genes (e.g., CFD, ECT2, HMMR) were classified as risk factors (Odds Ratio [OR] > 1), whereas ten genes (e.g., GALNT12, RMI1, VRK1) exhibited a protective effect (OR < 1). To visualize these associations, scatter plots, forest plots, and funnel plots were generated. Specifically, scatter plots for GALNT12, RMI1, and VRK1 (Fig. 3A) displayed a negative slope in their fitted regression lines, consistent with a protective association. Forest plots (Fig. 3B)

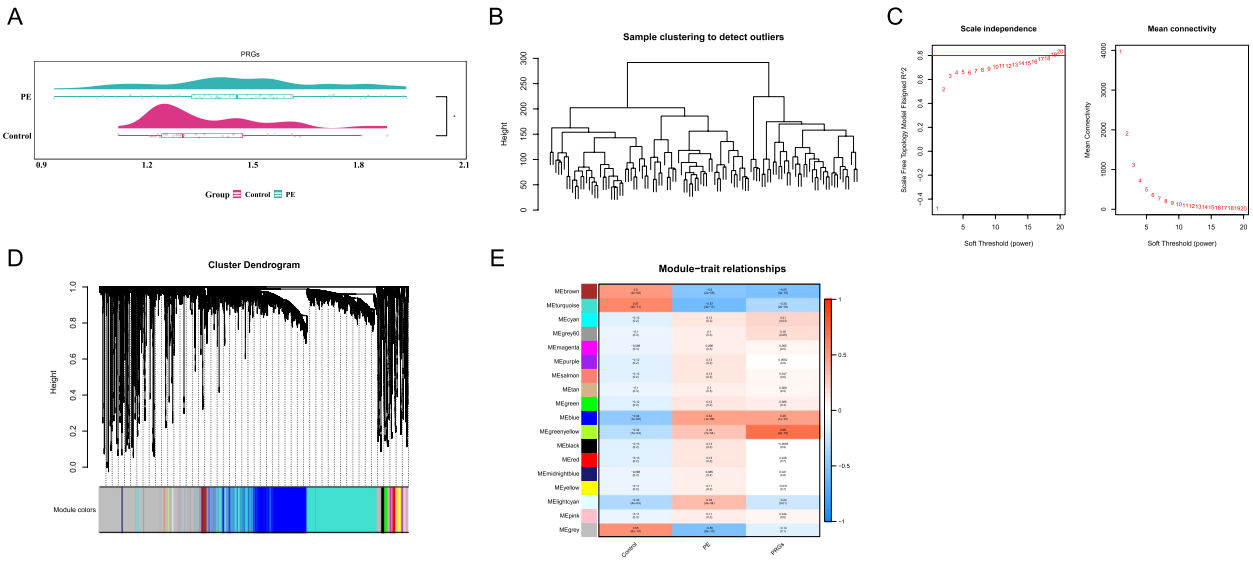

Fig. 1 Results of Screening palmitoacylation related gene modules. **A** The PRGs score of PE and control samples. **B** The result of cluster analysis. **C** The scale-free fit index for soft threshold power and mean connectivity. **D** Gene and trait clustering dendrograms. Each branch represents an expression module of a highly interconnected groups of genes; each color indicates a corresponding co-expression module. **E** Heatmap of 18 gene co-expression modules. The numbers in each cell means the correlation coefficient and *p* value

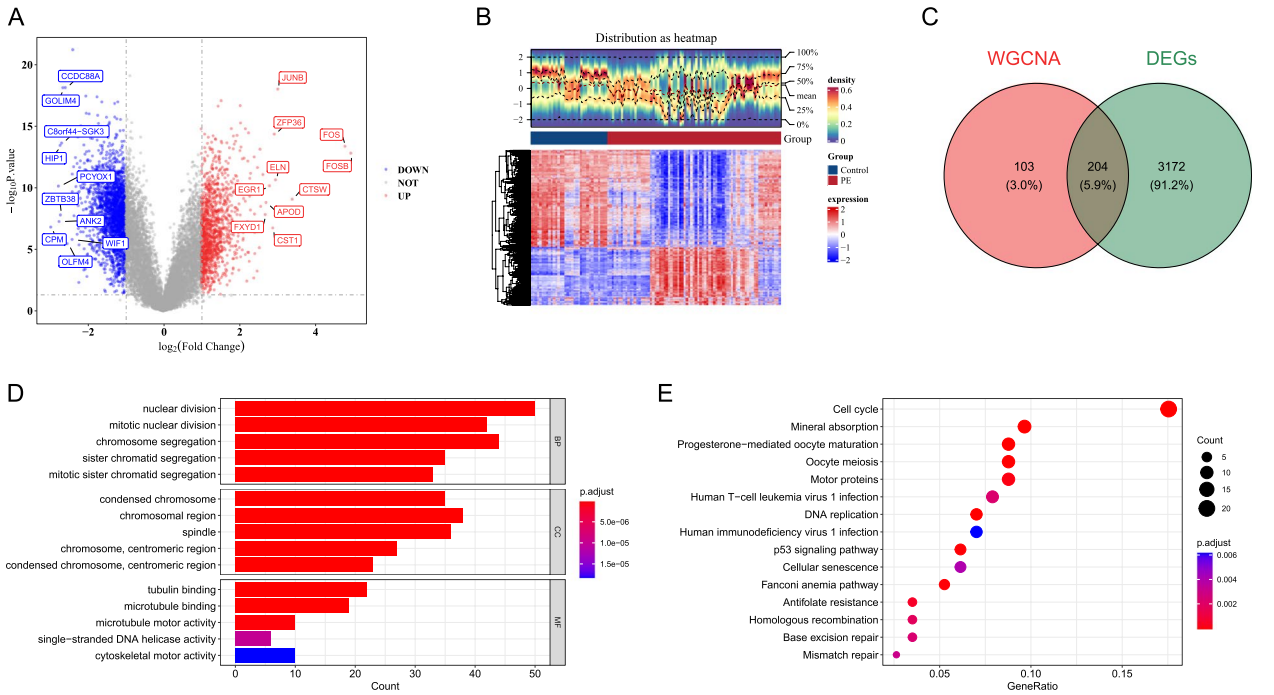

Fig. 2 Identification and functional exploration of the intersection genes. **A** Volcano plot. We set the criteria of |log2fold-change (FC)|> 1 and *P* < 0.05 as the difference genes. Red dots are upregulated genes, and blue dots are downregulated genes. **B** Heatmap plot. The heatmap reflects the distribution of gene expression density and gene expression differences in each sample. **C** Venn diagram. The key module genes obtained from WGCNA were intersected with DEGS genes. **D** GO enrichment analysis results. **E** KEGG enrichment analysis results

Table 1 Mendelian randomization analysis unveils 17 causal genes in endometriosis

NO	exposure	outcome	method	nsnp	pval	or
1	CENPE	PE	Inverse variance weighted	25	0.000458026	0.99892761
2	CFD	PE	Inverse variance weighted	7	0.013505093	1.000750339
3	ECT2	PE	Inverse variance weighted	11	0.049775503	1.000690854
4	FBXO5	PE	Inverse variance weighted	8	0.01256748	0.999008793
5	GALNT12	PE	Inverse variance weighted	9	0.011019426	0.998513982
6	HMMR	PE	Inverse variance weighted	5	0.008649861	1.002027803
7	IER3	PE	Inverse variance weighted	17	0.012138092	0.999591358
8	MKI67	PE	Inverse variance weighted	3	0.020648678	0.997693863
9	NDC80	PE	Inverse variance weighted	15	0.014084781	0.999332329
10	PARPBP	PE	Inverse variance weighted	4	0.003391087	0.997696177
11	PRIM1	PE	Inverse variance weighted	9	0.008881558	1.000353618
12	RLN2	PE	Inverse variance weighted	4	0.045332653	0.998816069
13	RMI1	PE	Inverse variance weighted	11	0.048692518	0.999587813
14	STIL	PE	Inverse variance weighted	16	0.009312601	1.000757596
15	STMN1	PE	Inverse variance weighted	19	0.00385043	1.000811607
16	TYMS	PE	Inverse variance weighted	12	0.002906875	1.00065104
17	VRK1	PE	Inverse variance weighted	10	0.002029756	0.999426071

Abbreviation: PE pelvic endometriosis

further illustrated the MR effect sizes, all of which were negative under the IVW method, reinforcing their protective role. Funnel plots (Fig. 3C) demonstrated a symmetrical distribution of IVs around the IVW line, indicating adherence to Mendel's second law. Scatter plots, forest plots, and funnel plots for the remaining

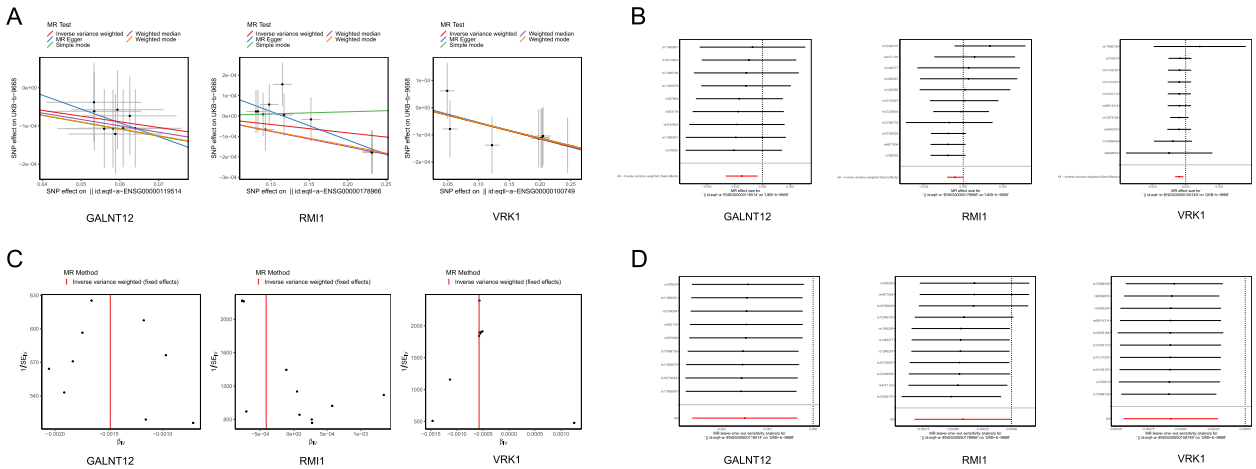

Fig. 3 Identification of candidate genes through MR study. **A** Scatter plots for GALNT12, RMI1, and VRK1. **B** Forest plots for GALNT12, RMI1, and VRK1. **C** Funnel plots for GALNT12, RMI1, and VRK1. **D** LOO analysis for GALNT12, RMI1, and VRK1

Table 2 Results of Mendelian randomization heterogeneity test

NO	exposure	outcome	heterogeneity_pval
1	CENPE	PE	0.994236723
2	CFD	PE	0.904994304
3	ECT2	PE	0.974875149
4	FBXO5	PE	0.856902477
5	GALNT12	PE	0.999813501
6	HMMR	PE	0.987296141
7	IER3	PE	0.414274668
8	MKI67	PE	0.935968918
9	NDC80	PE	0.999792808
10	PARPBP	PE	0.988250764
11	PRIM1	PE	0.946071659
12	RLN2	PE	0.925913532
13	RMI1	PE	0.659333301
14	STIL	PE	0.999978701
15	STMN1	PE	0.99963283
16	TYMS	PE	0.999579046
17	VRK1	PE	0.99775246

Abbreviation: PE pelvic endometriosis

Table 3 Results of Mendelian randomization level pleiotropy test

NO	exposure	outcome	pleiotropy_pval
1	CENPE	PE	0.159937324
2	CFD	PE	0.353849828
3	ECT2	PE	0.170419632
4	FBXO5	PE	0.612553883
5	GALNT12	PE	0.831829309
6	HMMR	PE	0.873546239
7	IER3	PE	0.053648145
8	MKI67	PE	0.791493743
9	NDC80	PE	0.975018594
10	PARPBP	PE	0.773482392
11	PRIM1	PE	0.362264287
12	RLN2	PE	0.808950553
13	RMI1	PE	0.070378789
14	STIL	PE	0.220005997
15	STMN1	PE	0.781020923
16	TYMS	PE	0.894010125
17	VRK1	PE	0.947229403

Abbreviation: PE pelvic endometriosis

genes are provided in Figures S1–S3. Additionally, heterogeneity and horizontal pleiotropy tests across all 17 genes yielded *P* values exceeding 0.05 (Tables 2 and 3), suggesting the absence of significant heterogeneity or confounding influences in the MR study. LOO analysis (Fig. 3D and Fig. S4) further corroborated the robustness of the MR results, as no substantial deviations were observed upon sequential exclusion of individual IVs. Finally, Steiger directionality tests (Table 4) confirmed the correct causal direction for all 17 genes, with *P* values below 0.05, reinforcing the validity of the findings. Collectively, these 17 genes emerge as potential causal candidates implicated in endometriosis.

VRK1, GALNT12, and RMI1 were deemed as key genes for endometriosis

Building on the 17 candidate genes identified through the MR study, machine learning algorithms were employed to further refine the selection of feature genes. Four distinct models were constructed, with their predictive performance assessed via ROC curves. All models

Table 4 Mendelian randomization Steiger directivity analysis

NO	exposure	outcome	correct_causal_direction	steiger_pval
1	CENPE	PE	TRUE	1.8803E- 163
2	CFD	PE	TRUE	< 0.001
3	ECT2	PE	TRUE	6.3846E- 150
4	FBXO5	PE	TRUE	8.09018E- 92
5	GALNT12	PE	TRUE	2.53764E- 52
6	HMMR	PE	TRUE	2.45247E- 33
7	IER3	PE	TRUE	< 0.001
8	MKI67	PE	TRUE	7.05518E- 18
9	NDC80	PE	TRUE	8.5987E- 214
10	PARPBP	PE	TRUE	4.02091E- 22
11	PRIM1	PE	TRUE	< 0.001
12	RLN2	PE	TRUE	3.27508E- 44
13	RMI1	PE	TRUE	< 0.001
14	STIL	PE	TRUE	2.468E- 171
15	STMN1	PE	TRUE	1.9595E- 242
16	TYMS	PE	TRUE	< 0.001
17	VRK1	PE	TRUE	< 0.001

Abbreviation: PE pelvic endometriosis

achieved an area under the curve (AUC) exceeding 0.7, indicative of high classification accuracy (Fig. 4A). Additionally, residual box plots compared true observed values with model-predicted outcomes, further validating model reliability (Fig. 4B). To prioritize genes with the greatest potential relevance to endometriosis treatment, gene importance scores were derived from each model (Fig. 4C). By selecting the top 10 genes from each model and determining their intersection, six feature genes were identified: TYMS, VRK1, MK167, GALNT12, CFD, and RMI1 (Fig. 4D).

Subsequent gene expression analysis in the GSE51981 and GSE25628 datasets revealed significantly lower expression levels of VRK1, GALNT12, and RMI1 in both datasets ($P < 0.05$) (Fig. 4E and F). Consequently, these three genes were designated as key genes implicated in endometriosis.

Immune cell infiltration analysis

Immune infiltration analysis (Fig. 5A) characterized the distribution of 22 immune cell types in endometriosis and control samples from GSE51981. The Wilcoxon test identified 11 differentially abundant immune cells. Notably, M2 macrophages and resting mast cells exhibited significantly higher proportions in control samples, whereas monocytes and resting natural killer (NK) cells were significantly enriched in endometriosis samples (Fig. 5B). Correlation analysis among immune cell populations demonstrated a strong positive association between resting mast cells and M0 macrophages ($r = 0.51$, $P < 0.05$), while regulatory T cells (Tregs) displayed the strongest negative correlation with activated memory CD4 T cells ($r = -0.53$, $P < 0.05$) (Fig. 5C). Further correlation

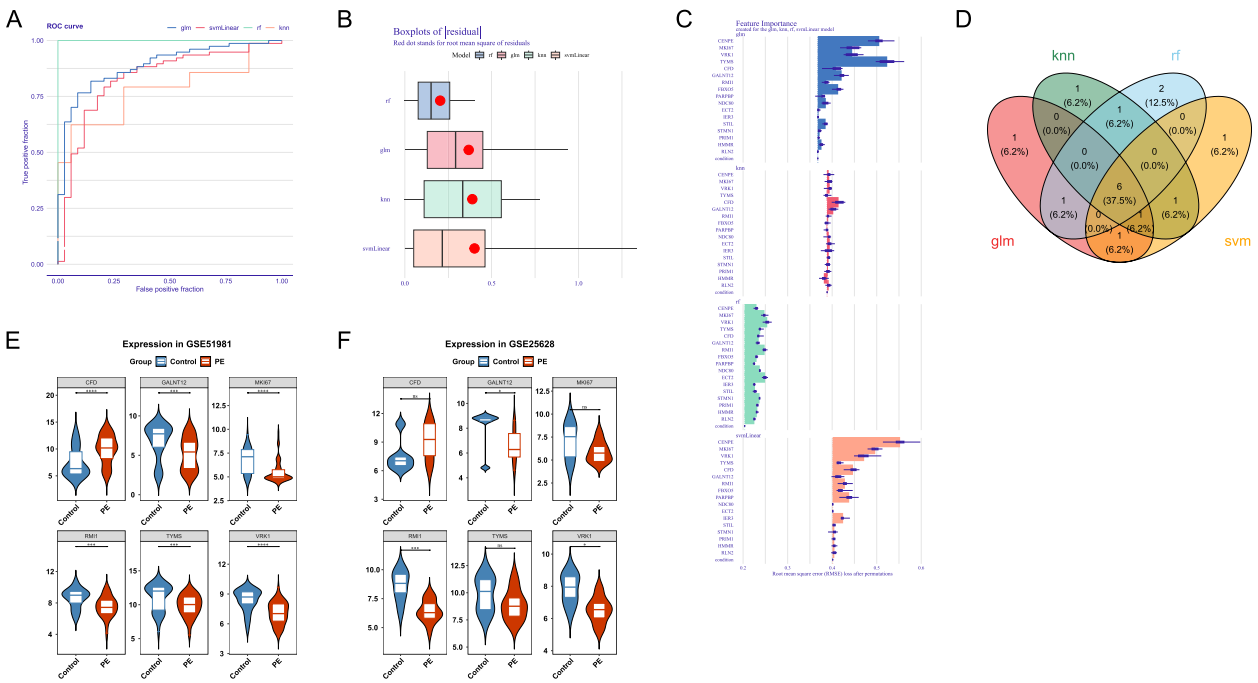

Fig. 4 Obtained key genes via machine learning and external validation. **A** ROC curves constructed by four machine learning models. **B** Residual box diagram of four machine learning models. **C** Feature importance of four machine learning models. **D** Venn diagram of the top 10 feature importance genes across four machine learning models. **E** Expression of feature genes in GSE51981. **F** Expression of feature genes in GSE25628

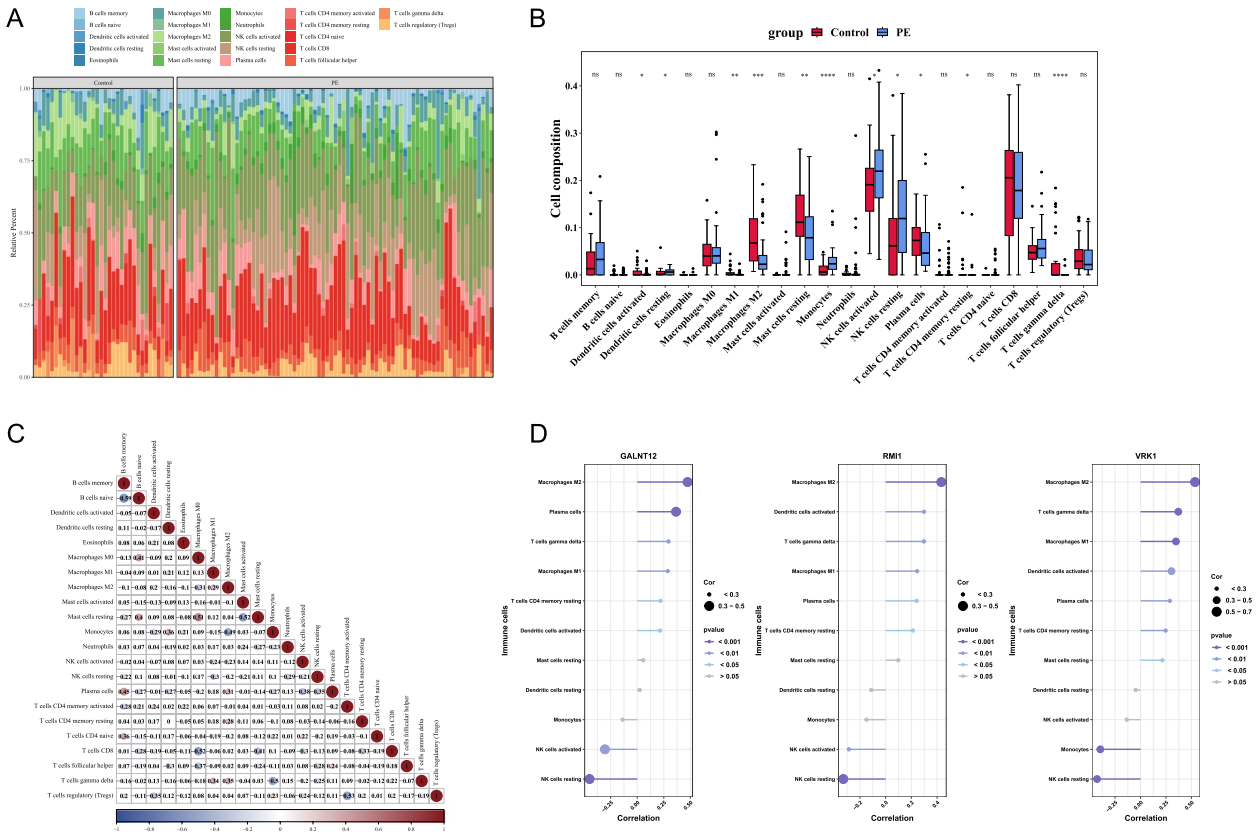

Fig. 5 Immune cell infiltration analysis. **A** Proportions of 22 immune cell types in PE and controls. **B** Expression differences of 22 immune cell types in PE and controls. **C** Relationships among immune cells. **D** Associations between immune cells and key genes

analysis between key genes and differentially abundant immune cells revealed a consistent positive association between all key genes and M2 macrophages, alongside a strong negative correlation with resting NK cells ($|r| > 0.3$, $P < 0.001$) (Fig. 5D).

Chromosome localization and functional similarity analysis of key genes

Chromosomal localization analysis provided further insights into the genomic context of the key genes. Specifically, GALNT12 and RMI1 were mapped to chromosome 9, whereas VRK1 was located on chromosome 14 (Fig. 6A). Functional similarity analysis revealed that VRK1 exhibited the highest similarity with the other key genes, suggesting its potential central role in the pathogenesis of endometriosis (Fig. 6B).

Analysis of regulatory networks associated with key genes

Prediction of miRNA interactions with key genes identified nine key miRNAs through overlapping results from the miRWalk and miRDB databases, enabling the construction of an mRNA-miRNA regulatory network comprising 12 nodes and 9 edges. Notable interactions included VRK1- 'hsa-mir- 4428', GALNT12- 'hsa-mir-202 -3p', and RMI1- 'hsa-mir- 3190 -3p' (Fig. 7A). Furthermore, 61 TFs targeting the three key genes were identified through overlapping predictions from the hTF-target and miRNet databases. These interactions were visualized in an mRNA-TF network consisting of 64 nodes (3 key genes and 61 TFs) and 76 edges, with SPI1 identified as a common regulator of all three key genes (Fig. 7B). Additionally, drug-gene interaction analysis identified 195 drugs targeting the three key genes, leading to the construction of a key gene-drug network (Fig. 7C). Notably, enterolactone was found to co-target RMI1 and VRK1, while retinoic acid co-targeted GALNT12 and VRK1. These regulatory networks provide valuable insights into the molecular mechanisms underlying endometriosis and potential therapeutic targets.

Validation of key genes by immunohistochemistry

To validate the expression patterns of the key genes, three cases of ectopic endometrial tissues and three cases of normal endometrial tissues were collected from the pathology department. Immunohistochemical staining was performed using antibodies against VRK1, RMI1,

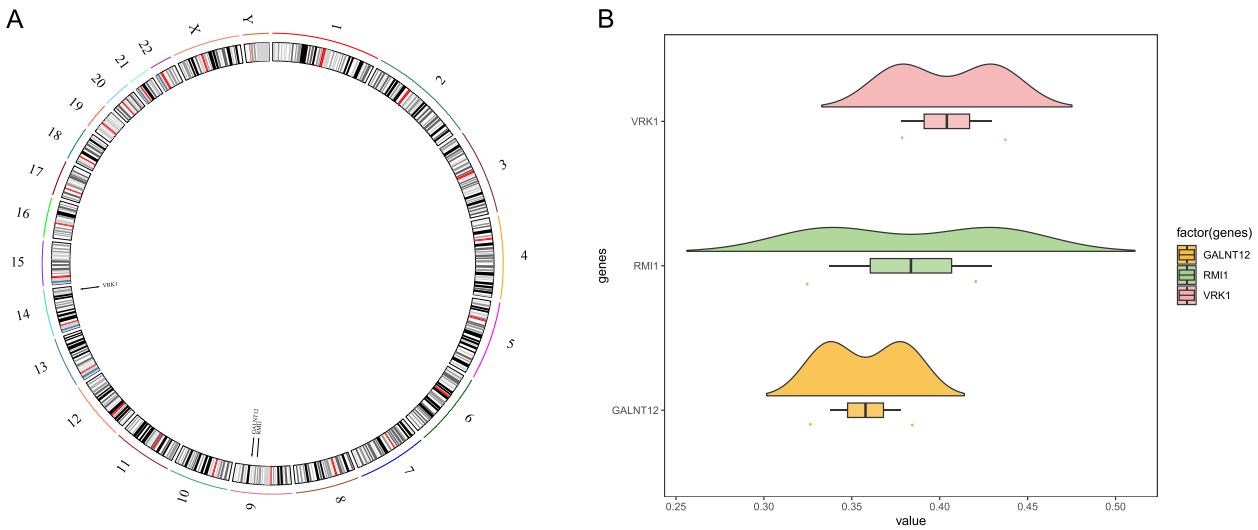

Fig. 6 Chromosome localization and functional similarity analysis of key genes. **A** The chromosome localization of key genes. **B** The functional similarity analysis of key genes

and GALNT12. The results demonstrated significantly higher positive staining rates for all three proteins in normal endometrial tissues compared to endometriotic tissues, further corroborating their potential involvement in endometriosis pathophysiology (Fig. 8).

Discussion

Endometriosis is an inflammatory disease characterized by invasiveness and recurrence, and currently lacks reliable diagnostic and monitoring indicators [2, 4]. Palmitoylation stands as a pivotal mechanism of protein post-translational modification, exerting a significant influence on inflammatory responses, lipid metabolism, and the genesis of tumors [12, 45]. Research indicates that palmitoylation plays a significant role in the migration and adhesion of neutrophils by regulating the function of CRACR2 A protein, thereby affecting inflammatory responses and associated tissue damage [46]. Additionally, palmitoylation plays an important role in inflammatory responses by modulating the functions of immune proteins and the metabolism of gut microbiota [47]. Although the specific role of palmitoylation in endometriosis remains unclear, its close association with inflammation suggests that it may play a key role in the inflammatory process of this disease. This study employed bioinformatics approaches to identify DEGs associated with palmitoylation in endometriosis and further elucidated their functional relevance. Using the IEU OpenGWAS database, 17 genes were identified with statistically significant associations, establishing a causal relationship between these genes and endometriosis. Subsequently, machine learning algorithms, combined with external dataset validation, refined this selection to three key genes—VRK1, GALNT12, and RMI1—each exhibiting reduced expression in endometriotic tissues and demonstrating a negative correlation with disease occurrence.

The VRK1 (vaccinia-related kinase 1) gene, which encodes a serine/threonine protein kinase, is localized on chromosome 14 and exhibits broad expression across human tissues, with predominant nuclear localization [48]. The VRK1-encoded protein regulates cell cycle progression and genomic stability through phosphorylation and is implicated in apoptosis, thus contributing to cellular proliferation and tissue regeneration [49]. Previous studies have demonstrated that VRK1 modulates p53 stability and activity via phosphorylation, thereby influencing lung cancer cell proliferation [50]. Additionally, VRK1 promotes cell cycle progression by phosphorylating VREB, thereby enhancing cAMP-responsive element-binding protein activity at the CCND1 promoter, leading to CCND1 upregulation [51]. Furthermore, VRK1 plays a pivotal role in DNA damage repair by stabilizing histone H2 AX-H3 interactions, neutralizing ionizing radiation-induced H2 AX phosphorylation, and participating in early DNA repair mechanisms [52].

The GALNT12 (N-Acetylgalactosaminyltransferase 12) gene, located on chromosome 9, belongs to the polypeptide N-acetylgalactosaminyltransferase family and is primarily involved in protein post-translational modification. It catalyzes the transfer of N-acetylgalactosamine to serine or threonine residues of target proteins, thereby influencing protein conformation, functional

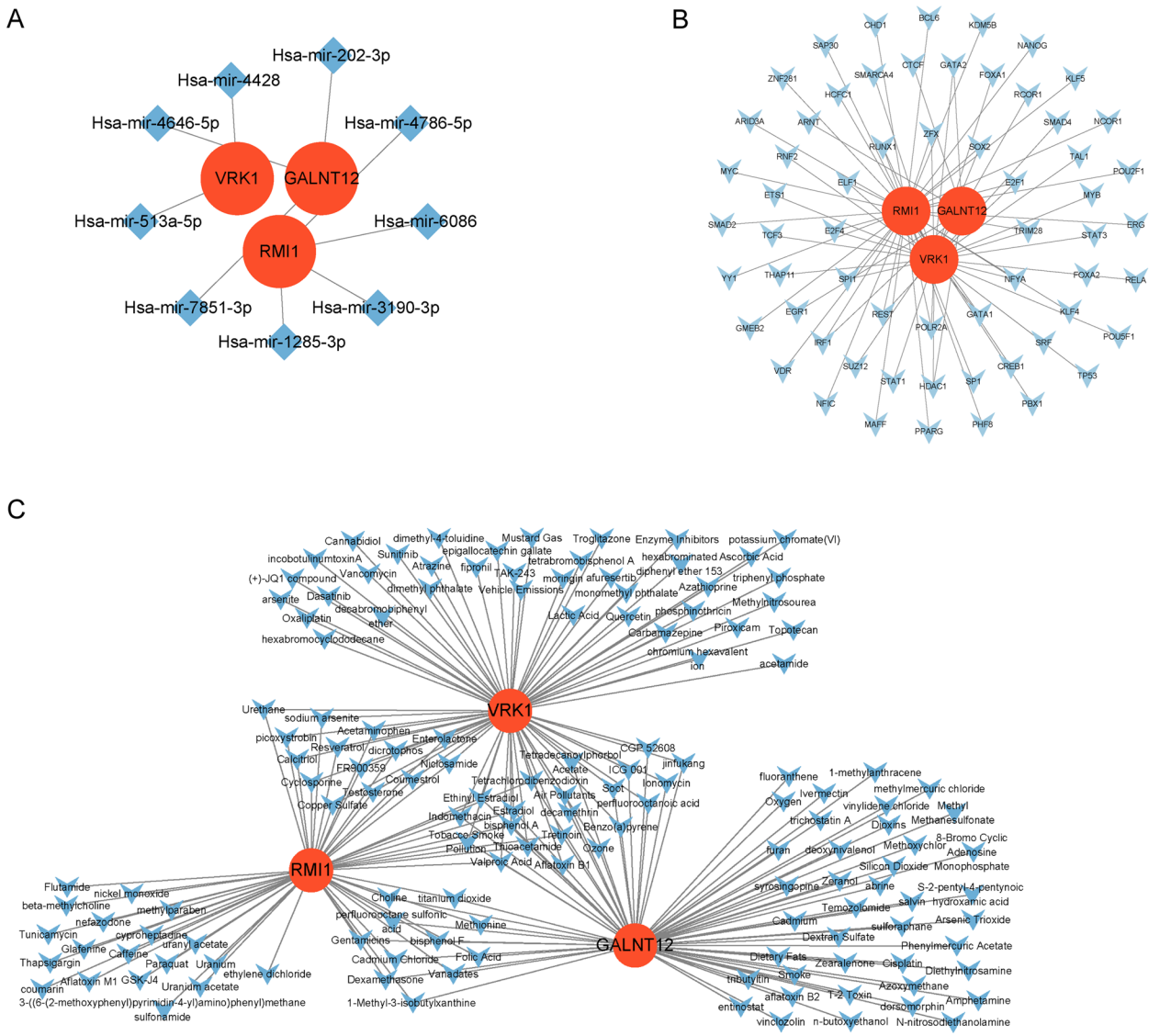

Fig. 7 The regulatory networks associated with key genes. **A** The mRNA-miRNA network of key genes. **B** The mRNA-TF network of key genes. **C** The key genes-drugs network

properties, and genomic stability [53]. Aberrant expression or dysregulation of GALNT12 has been implicated in various pathological conditions. For instance, mutations in GALNT12 leading to abnormal glycosylation play a critical role in the pathogenesis of colorectal cancer [54]. Moreover, elevated GALNT12 expression is significantly associated with poor prognosis in patients with glioblastoma, where it enhances tumor cell proliferation and invasiveness via modulation of the PI3 K/AKT/mTOR signaling pathway [55]. Additionally, GALNT12 has been closely linked to IgA1 galactose deficiency, with significantly lower mRNA expression levels observed in affected individuals compared to healthy controls [56].

The RMI1 (RecQ Mediated Genome Instability 1) gene, also localized on chromosome 9, encodes a key protein involved in DNA repair and recombination. As an integral component of the BLM/RMI1/Top3α complex, RMI1 plays a pivotal role in maintaining genomic stability and facilitating DNA damage repair [57]. Loss of RMI1 function leads to increased DNA damage accumulation, cell cycle arrest, and impaired homologous recombination repair, particularly following ionizing radiation exposure [58]. Beyond its role in genomic maintenance, RMI1 is involved in metabolic regulation, with its expression in adipocytes being modulated by glucose through the E2 F pathway [59]. RMI1-deficient

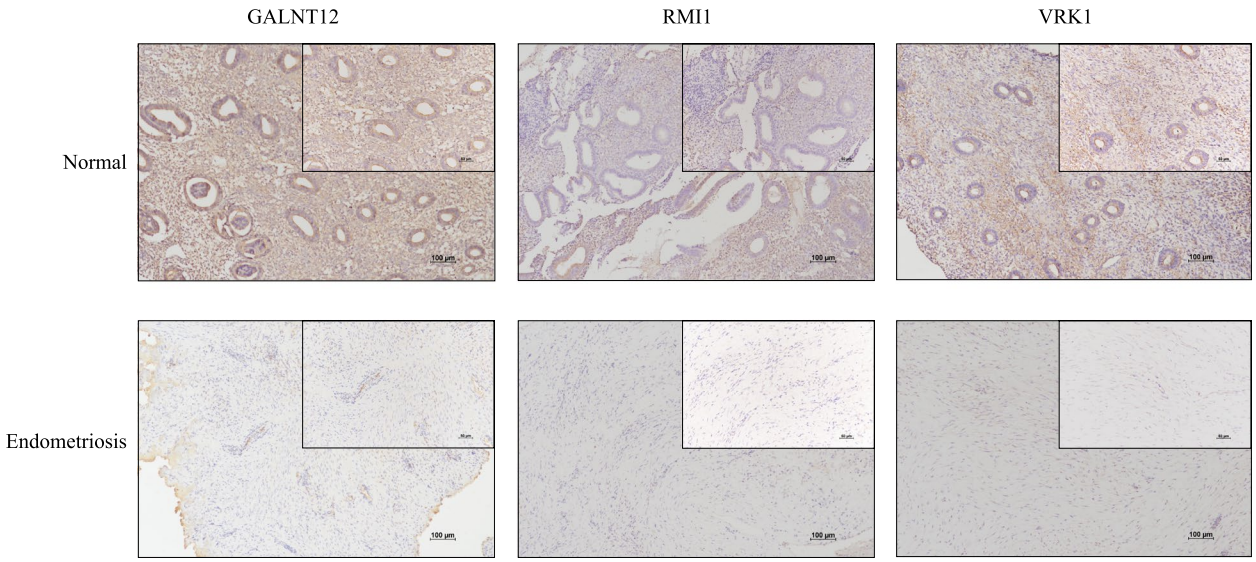

Fig. 8 Immunohistochemical Validation of GALNT12, RMI1 and VRK1 in Normal and Endometriosis

mice exhibit resistance to diet- and genetically induced obesity, highlighting its involvement in metabolic homeostasis [60]. Furthermore, mutations in RMI1 contribute to the pathogenesis of Bloom syndrome, a genetic disorder characterized by primary microcephaly, intrauterine growth restriction, and short stature [61].

Although direct evidence linking GALNT12, RMI1, and VRK1 to endometriosis remains limited, their well-documented roles in gene expression regulation, cell signaling, DNA repair, cell cycle progression, and apoptosis suggest potential involvement in the disease's pathogenesis. For instance, mutations in GALNT12 or RMI1 leading to aberrant protein function may compromise the stability and proliferative capacity of endometrial cells. Simultaneously, dysregulated VRK1 activity could disrupt normal cell cycle control, potentially contributing to the onset and progression of endometriosis.

Immunofiltration analysis identified 11 distinct immune cell types exhibiting differential infiltration patterns in endometriosis. Notably, M2 macrophages demonstrated reduced abundance in endometriotic tissues, whereas resting NK cells were significantly enriched. M2 macrophages are recognized for their role in tissue repair, angiogenesis, and tumor progression [62]. Prior studies have reported a marked decline in M2 macrophage proportions across all stages of endometriosis in affected individuals [63]. Consistent with these findings, the key genes identified in this study were downregulated in ectopic endometrial tissues and exhibited a positive correlation with M2 macrophage infiltration. NK cells, as critical components of the innate immune system, contribute to immune surveillance and tissue homeostasis. Within the endometrium, a specialized subset known as uterine NK (uNK) cells has been identified [64]. Research indicates that $CD16^{+}$ uNK cells produce cytotoxic factors capable of affecting trophoblast function, potentially leading to infertility, miscarriage, or placental abnormalities [65]. While this study observed a negative correlation between key genes and resting NK cells, alongside increased NK cell infiltration in ectopic endometrial tissues, the precise role of NK cells in endometriosis remains inconclusive [66]. Further investigation with larger sample cohorts and additional functional validation is required.

MicroRNAs (miRNAs), a class of short non-coding RNAs, regulate gene expression post-transcriptionally by modulating mRNA stability and translation efficiency. Aberrant miRNA expression has been extensively documented in endometriosis. This study predicted miRNA interactions with the three key genes, highlighting miR- 202, which has been reported to be upregulated in ectopic endometrial tissue. Notably, miR- 202 suppresses SOX6 expression, thereby enhancing the invasive capacity of ectopic endometrial cells [67]. Although the miRNAs identified in this study have not been directly investigated in endometriosis, their involvement in other pathological conditions has been documented. In cervical cancer, RGMB-AS1 promotes tumor proliferation and invasiveness via the miR- 4428/PBX1 axis [68], while in ovarian cancer, miR- 6086 suppresses angiogenesis by downregulating the OC2/VEGFA/EGFL6 signaling pathway [69]. Within the mRNA-TF regulatory network, SPI1

was identified as a shared transcriptional regulator of the three key genes. Notably, SPI1 is upregulated in ectopic endometrial tissues, contributing to the aggressive phenotype of endometriotic lesions [70]. Furthermore, drug repurposing analysis using the CTD and Enrichr databases identified 195 drug candidates targeting the key genes. This network encompasses a diverse range of therapeutic agents, including retinoic acid, which has demonstrated potential for endometriosis treatment by inhibiting estradiol secretion in ovarian endometriotic cysts and attenuating disease progression [71]. Additionally, while enterolactones have not been studied in the context of endometriosis, their therapeutic potential in other malignancies has been explored. Specifically, enterolactones have been shown to enhance radiotherapy efficacy in breast cancer by inhibiting DNA repair mechanisms and promoting apoptotic pathways [72].

The mechanisms underlying targeted drug actions are highly intricate, with potential impacts on disease progression mediated through diverse pathways. While most studies suggest that targeted therapies exert their effects primarily by downregulating the expression of target genes [73, 74], their functional scope extends beyond mere gene suppression. For example, TP53 serves as a pivotal tumor suppressor gene, and its functional loss is implicated in the pathogenesis of numerous malignancies. Restoring TP53 activity via targeted therapies can reestablish its antitumor function, thereby inhibiting tumor progression [75]. Similarly, FoxP3, a key transcription factor essential for the development and function of Tregs, plays a critical role in immune modulation. Upregulation of FoxP3 enhances the immunosuppressive capacity of Tregs, influencing the onset and progression of esophageal cancer [76]. Given the multifaceted mechanisms of targeted drugs, identifying effective therapeutic targets is imperative for advancing treatment strategies, improving clinical outcomes, and improving patient prognosis.

This study has inherent limitations stemming from its reliance on data sourced from multiple public databases, which may introduce potential biases. Furthermore, the analysis is predominantly bioinformatics-driven, lacking extensive experimental validation. Although preliminary immunohistochemical analysis corroborated the computational findings regarding the expression of key genes in tissue samples, additional validation is required. Future work will focus on quantifying gene expression using Western blot and quantitative polymerase chain reaction (qPCR) methodologies. Moreover, functional assays will be conducted at the cellular level, including gene overexpression experiments to assess the impact of these genetic alterations on cell proliferation, migration, invasion, and apoptosis.

Conclusions

Overall, this study employed an integrative approach combining differential gene expression analysis, WGCNA, MR analysis, and machine learning to identify three key genes associated with palmitoylation in endometriosis. Subsequent analyses explored immune infiltration dynamics, gene functional similarity, and pharmacological correlations. These findings provide novel insights that may inform clinical diagnostics, disease surveillance, and therapeutic development for endometriosis.

Abbreviations

MR	Mendelian Randomization
GEO	Gene Expression Omnibus
GWAS	Genome-Wide Association Studies
PE	Pelvic endometriosis
IEU	Integrative Epidemiology Unit
SNPs	Single nucleotide polymorphisms
PRGs	Palmitoylation relacated genes
WGCNA	Weighted Gene Co-expression Network Analysis
ssGSEA	Single-sample gene set enrichment analysis
DEGs	Differentially expressed genes
GO	Gene Ontology
KEGG	Kyoto Encyclopedia of Genes and Genomes
BP	Biological process
CC	Cellular component
MF	Molecular function
IVs	Instrumental variables
LD	Linkage disequilibrium
IVW	Inverse Variance Weighted
LOO	Leave-one-out
RF	Random Forest
SVM	Support Vector Machine
GLM	Generalized Linear Model
KNN	K-Nearest Neighbor
ROC	Receiver operating characteristic
AUC	Area under the curve
CTD	Comparative toxicogenomics
NK	Nature killer
Tregs	Regulatory T cells
UCSC	University of California Santa Cruz
TFs	Transcription factors
uNK	Uterine natural killer
IHC	Immunohistochemistry.
FC	Fold Change
qPCR	Quantitative Polymerase Chain Reaction

Supplementary Information

The online version contains supplementary material available at https://doi.org/10.1186/s12905-025-03697-0.

Supplementary Material 1.

Acknowledgements

The authors would like to express their gratitude to the generous contributors of the GEO and GWAS databases for sharing their valuable data.

Authors' contributions

Q. C. and J. F. designed the thesis. J. K. carried out the study data analysis and contributed to the writing-original draft, review & editing. J. S. contributed in the calibration of the data and the figures. Y. Y. contributed in the software and hardware maintenance. X. L. contributed to assist in writing-original draft, review & editing. H. H. managed the typesetting of the manuscript. All authors have read and approved the final version of the manuscript.

Funding
This work was supported by the National Natural Science Foundation of China (No. 82104908).

Data availability
All data generated or analysed during this study are included in this published article and its supplementary information files. The datasets used for analysis in this paper are derived from GEO (https://www.ncbi.nlm.nih.gov/gds) and IEU OpenGWAS (https://gwas.mrcieu.ac.uk/) databases.

Declarations

Ethics approval and consent to participate
The study was approved by Shanghai General Hospital Institutional Review Board. The approval number is 20240711101424110.

Consent for publication
Not applicable.

Competing interests
The authors declare no competing interests.

Author details
[1]Department of Clinical Medical Laboratory, The Affiliated Second Hospital of Xiamen Medical College, Xiamen, Fujian, China. [2]Department of Pathology, The Affiliated Second Hospital of Xiamen Medical College, Xiamen, Fujian, China. [3]Department of Microbiology, Guilin Medical University, Guilin, Guangxi, China. [4]Department of Laboratory Medicine, Shanghai General Hospital, Shanghai Jiao Tong University School of Medicine, Shanghai, China. [5]Department of Traditional Chinese Medicine, Shanghai General Hospital, Shanghai Jiao Tong University School of Medicine (Originally Named "Shanghai First People's Hospital"), Shanghai, China.

Received: 31 August 2024 Accepted: 28 March 2025
Published online: 05 April 2025

References

1. Allaire C, Bedaiwy MA, Yong PJ. Diagnosis and management of endometriosis. Can Med ASsoc J. 2023;195(10):E363–71.
2. Symons LK, Miller JE, Kay VR, Marks RM, Liblik K, Koti M, Tayade C. The Immunopathophysiology of Endometriosis. Trends Mol Med. 2018;24(9):748–62.
3. Nnoaham KE, Hummelshoj L, Webster P, D'Hooghe T, de Cicco NF, de Cicco NC, Jenkinson C, Kennedy SH, Zondervan KT. Impact of endometriosis on quality of life and work productivity: a multicenter study across ten countries. Fertil Steril. 2011;96(2):366–73.
4. Burney RO, Giudice LC. Pathogenesis and pathophysiology of endometriosis. Fertil Steril. 2012;98(3):511–9.
5. Sanchez AM, Viganò P, Somigliana E, Cioffi R, Panina-Bordignon P, Candiani M. The endometriotic tissue lining the internal surface of endometrioma: hormonal, genetic, epigenetic status, and gene expression profile. Reprod Sci. 2015;22(4):391–401.
6. Reis FM, Petraglia F, Taylor RN. Endometriosis: hormone regulation and clinical consequences of chemotaxis and apoptosis. Hum Reprod Update. 2013;19(4):406–18.
7. Leyland N, Casper R, Laberge P, Singh SS. Endometriosis: diagnosis and management. J Obstet Gynaecol CA. 2010;32(7 Suppl 2):S1–32.
8. Bedaiwy MA, Allaire C, Alfaraj S. Long-term medical management of endometriosis with dienogest and with a gonadotropin-releasing hormone agonist and add-back hormone therapy. Fertil Steril. 2017;107(3):537–48.
9. Donnez J, Squifflet J. Complications, pregnancy and recurrence in a prospective series of 500 patients operated on by the shaving technique for deep rectovaginal endometriotic nodules. Hum Reprod. 2010;25(8):1949–58.
10. Gu M, Jiang H, Tan M, Yu L, Xu N, Li Y, Wu H, Hou Q, Dai C. Palmitoyltransferase DHHC9 and acyl protein thioesterase APT1 modulate renal fibrosis through regulating β-catenin palmitoylation. Nat Commun. 2023;14(1):6682.
11. Chamberlain LH, Shipston MJ. The physiology of protein S-acylation. Physiol Rev. 2015;95(2):341–76.
12. Wang L, Cui J. Palmitoylation promotes chaperone-mediated autophagic degradation of NLRP3 to modulate inflammation. Autophagy. 2023;19(10):2821–3.
13. Zhou L, He X, Wang L, Wei P, Cai Z, Zhang S, Jin S, Zeng H, Cui J. Palmitoylation restricts SQSTM1/p62-mediated autophagic degradation of NOD2 to modulate inflammation. Cell Death Differ. 2022;29(8):1541–51.
14. Zhang M, Shi Z, Peng X, Cai D, Peng R, Lin Y, Dai L, Li J, Chen Y, Xiao J, et al. NLRP3 inflammasome-mediated Pyroptosis induce Notch signal activation in endometriosis angiogenesis. Mol Cell Endocrinol. 2023;574: 111952.
15. Nishimoto-Kakiuchi A, Sato I, Nakano K, Ohmori H, Kayukawa Y, Tanimura H, Yamamoto S, Sakamoto Y, Nakamura G, Maeda A et al: A long-acting anti-IL-8 antibody improves inflammation and fibrosis in endometriosis. Sci Transl Med 2023, 15(684):eabq5858.
16. Huang Y, Huang Y, Cai Z, Ferrari MW, Li C, Zhang T, Lyu G, Wang Z. MiR-21-3p inhibitor exerts myocardial protective effects by altering macrophage polarization state and reducing excessive mitophagy. Commun Biol. 2024;7(1):1371.
17. Yang S, Li M, Lian G, Wu Y, Cui J, Wang L: ABHD8 antagonizes inflammation by facilitating chaperone-mediated autophagy-mediated degradation of NLRP3. Autophagy 2024:1–14.
18. Nie L, Fei C, Fan Y, Dang F, Zhao Z, Zhu T, Wu X, Dai T, Balasubramanian A, Pan J, et al. Consecutive palmitoylation and phosphorylation orchestrates NLRP3 membrane trafficking and inflammasome activation. Mol Cell. 2024;84(17):3336–53.
19. Zhu XX, Meng XY, Zhang AY, Zhao CY, Chang C, Chen TX, Huang YB, Xu JP, Fu X, Cai WW, et al. Vaccarin alleviates septic cardiomyopathy by potentiating NLRP3 palmitoylation and inactivation. Phytomedicine. 2024;131: 155771.
20. Koster KP, Fyke Z, Nguyen T, Niqula A, Noriega-González LY, Woolfrey KM, Dell'Acqua ML, Cologna SM, Yoshii A. Akap5 links synaptic dysfunction to neuroinflammatory signaling in a mouse model of infantile neuronal ceroid lipofuscinosis. Front Synaptic Neuro. 2024;16:1384625.
21. Zhou B, Hao Q, Liang Y, Kong E. Protein palmitoylation in cancer: molecular functions and therapeutic potential. Mol Oncol. 2023;17(1):3–26.
22. Hänzelmann S, Castelo R, Guinney J. GSVA: gene set variation analysis for microarray and RNA-seq data. BMC Bioinformatics. 2013;14:7.
23. Langfelder P, Horvath S. WGCNA: an R package for weighted correlation network analysis. BMC Bioinformatics. 2008;9:559.
24. Ritchie ME, Phipson B, Wu D, Hu Y, Law CW, Shi W, Smyth GK. limma powers differential expression analyses for RNA-sequencing and microarray studies. Nucleic Acids Res. 2015;43(7): e47.
25. Gustavsson EK, Zhang D, Reynolds RH, Garcia-Ruiz S, Ryten M. ggtranscript: an R package for the visualization and interpretation of transcript isoforms using ggplot2. Bioinformatics. 2022;38(15):3844–6.
26. Gu Z. Complex heatmap visualization Imeta. 2022;1(3): e43.
27. Yu G, Wang LG, Han Y, He QY. clusterProfiler: an R package for comparing biological themes among gene clusters. OMICS. 2012;16(5):284–7.
28. Zhou H, Zhang Y, Liu J, Yang Y, Fang W, Hong S, Chen G, Zhao S, Zhang Z, Shen J, et al. Education and lung cancer: a Mendelian randomization study. Int J Epidemiol. 2019;48(3):743–50.
29. Obenchain V, Lawrence M, Carey V, Gogarten S, Shannon P, Morgan M. VariantAnnotation: a Bioconductor package for exploration and annotation of genetic variants. Bioinformatics. 2014;30(14):2076–8.
30. Hemani GEBP: ieugwasr: Interface to the "OpenGWAS" Database API. R package version 1.0.1 edition.; 2024.
31. Bowden J, Davey SG, Burgess S. Mendelian randomization with invalid instruments: effect estimation and bias detection through Egger regression. Int J Epidemiol. 2015;44(2):512–25.
32. Bowden J, Davey SG, Haycock PC, Burgess S. Consistent Estimation in Mendelian Randomization with Some Invalid Instruments Using a Weighted Median Estimator. Genet Epidemiol. 2016;40(4):304–14.
33. Burgess S, Butterworth A, Thompson SG. Mendelian randomization analysis with multiple genetic variants using summarized data. Genet Epidemiol. 2013;37(7):658–65.

34. Hemani G, Zheng J, Elsworth B, Wade KH, Haberland V, Baird D, Laurin C, Burgess S, Bowden J, Langdon R et al: The MR-Base platform supports systematic causal inference across the human phenome. Elife 2018, 7.
35. Hartwig FP, Davey SG, Bowden J. Robust inference in summary data Mendelian randomization via the zero modal pleiotropy assumption. Int J Epidemiol. 2017;46(6):1985–98.
36. Lu L, Wan B, Li L, Sun M. Hypothyroidism has a protective causal association with hepatocellular carcinoma: A two-sample Mendelian randomization study. Front Endocrinol. 2022;13: 987401.
37. Verbanck M, Chen CY, Neale B, Do R. Detection of widespread horizontal pleiotropy in causal relationships inferred from Mendelian randomization between complex traits and diseases. Nat Genet. 2018;50(5):693–8.
38. Jin T, Huang W, Cao F, Yu X, Guo S, Ying Z, Xu C. Causal association between systemic lupus erythematosus and the risk of dementia: A Mendelian randomization study. Front Immunol. 2022;13:1063110.
39. Van Essen DC. Cortical cartography and Caret software. Neuroimage. 2012;62(2):757–64.
40. Guan C, Ma F, Chang S, Zhang J. Interpretable machine learning models for predicting venous thromboembolism in the intensive care unit: an analysis based on data from 207 centers. Crit Care. 2023;27(1):406.
41. Chen B, Khodadoust MS, Liu CL, Newman AM, Alizadeh AA. Profiling Tumor Infiltrating Immune Cells with CIBERSORT. Methods Mol Biol. 2018;1711:243–59.
42. Zhang H, Meltzer P, Davis S. RCircos: an R package for Circos 2D track plots. BMC Bioinformatics. 2013;14:244.
43. Yang L, Yu X, Liu M, Cao Y. A comprehensive analysis of biomarkers associated with synovitis and chondrocyte apoptosis in osteoarthritis. Front Immunol. 2023;14:1149686.
44. Shannon P, Markiel A, Ozier O, Baliga NS, Wang JT, Ramage D, Amin N, Schwikowski B, Ideker T. Cytoscape: a software environment for integrated models of biomolecular interaction networks. Genome Res. 2003;13(11):2498–504.
45. Zhao L, Zhang C, Luo X, Wang P, Zhou W, Zhong S, Xie Y, Jiang Y, Yang P, Tang R, et al. CD36 palmitoylation disrupts free fatty acid metabolism and promotes tissue inflammation in non-alcoholic steatohepatitis. J Hepatol. 2018;69(3):705–17.
46. Lee J, Balzraine B, Schweizer A, Kuzmanova V, Gwack Y, Razani B, Lee JM, Mosher DF, Cho J: Neutrophil CRACR2A Promotes Neutrophil Recruitment in Sterile Inflammation and Ischemic Stroke. Circulation 2024.
47. Ma Y, Chen Y, Li L, Wu Z, Cao H, Zhu C, Liu Q, Wang Y, Chen S, Liu Y et al: 2-Bromopalmitate-Induced Intestinal Flora Changes and Testicular Dysfunction in Mice. Int J Mol Sci 2024, 25(21).
48. Manning G, Whyte DB, Martinez R, Hunter T, Sudarsanam S. The protein kinase complement of the human genome. Science. 2002;298(5600):1912–34.
49. Budziszewski GR, Zhao Y, Spangler CJ, Kedziora KM, Williams MR, Azzam DN, Skrajna A, Koyama Y, Cesmat AP, Simmons HC, et al. Multivalent DNA and nucleosome acidic patch interactions specify VRK1 mitotic localization and activity. Nucleic Acids Res. 2022;50(8):4355–71.
50. Vega FM, Sevilla A, Lazo PA. p53 Stabilization and accumulation induced by human vaccinia-related kinase 1. Mol Cell Biol. 2004;24(23):10366–80.
51. Kang TH, Park DY, Kim W, Kim KT. VRK1 phosphorylates CREB and mediates CCND1 expression. J Cell SCI. 2008;121(Pt 18):3035–41.
52. Salzano M, Sanz-García M, Monsalve DM, Moura DS, Lazo PA. VRK1 chromatin kinase phosphorylates H2AX and is required for foci formation induced by DNA damage. Epigenetics-US. 2015;10(5):373–83.
53. Ping X, Stark JM. O-GlcNAc transferase is important for homology-directed repair. DNA Repair. 2022;119: 103394.
54. Guda K, Moinova H, He J, Jamison O, Ravi L, Natale L, Lutterbaugh J, Lawrence E, Lewis S, Willson JK, et al. Inactivating germ-line and somatic mutations in polypeptide N-acetylgalactosaminyltransferase 12 in human colon cancers. P Natl Acad Sci USA. 2009;106(31):12921–5.
55. Zheng Y, Liang M, Wang B, Kang L, Yuan Y, Mao Y, Wang S. GALNT12 is associated with the malignancy of glioma and promotes glioblastoma multiforme in vitro by activating Akt signaling. Biochem Bioph res CO. 2022;610:99–106.
56. Wang YN, Zhou XJ, Chen P, Yu GZ, Zhang X, Hou P, Liu LJ, Shi SF, Lv JC, Zhang H. Interaction between GALNT12 and C1GALT1 Associates with Galactose-Deficient IgA1 and IgA Nephropathy. J Am Soc Nephrol. 2021;32(3):545–52.
57. Yang J, O'Donnell L, Durocher D, Brown GW. RMI1 promotes DNA replication fork progression and recovery from replication fork stress. Mol Cell Biol. 2012;32(15):3054–64.
58. Fang L, Sun Y, Dong M, Yang M, Hao J, Li J, Zhang H, He N, Du L, Xu C. RMI1 facilitates repair of ionizing radiation-induced DNA damage and maintenance of genomic stability. Cell Death Discov. 2023;9(1):426.
59. Suwa A, Yoshino M, Kurama T, Shimokawa T, Aramori I. Glucose regulates RMI1 expression through the E2F pathways in adipose cells. Endocrine. 2011;40(1):56–61.
60. Suwa A, Yoshino M, Yamazaki C, Naitou M, Fujikawa R, Matsumoto S, Kurama T, Shimokawa T, Aramori I. RMI1 deficiency in mice protects from diet and genetic-induced obesity. Febs J. 2010;277(3):677–86.
61. Gönenc II, Elcioglu NH, Martinez GC, Aras S, Großmann N, Praulich I, Altmüller J, Kaulfuß S, Li Y, Nürnberg P, et al. Phenotypic spectrum of BLM- and RMI1-related Bloom syndrome. Clin Genet. 2022;101(5–6):559–64.
62. Mantovani A, Sozzani S, Locati M, Allavena P, Sica A. Macrophage polarization: tumor-associated macrophages as a paradigm for polarized M2 mononuclear phagocytes. Trends Immunol. 2002;23(11):549–55.
63. Takebayashi A, Kimura F, Kishi Y, Ishida M, Takahashi A, Yamanaka A, Wu D, Zheng L, Takahashi K, Suginami H, et al. Subpopulations of macrophages within eutopic endometrium of endometriosis patients. Am J Reprod Immunol. 2015;73(3):221–31.
64. Thiruchelvam U, Wingfield M, O'Farrelly C. Increased uNK Progenitor Cells in Women With Endometriosis and Infertility are Associated With Low Levels of Endometrial Stem Cell Factor. Am J Reprod Immunol. 2016;75(4):493–502.
65. Lee SK, Kim CJ, Kim DJ, Kang JH. Immune cells in the female reproductive tract. Immune Netw. 2015;15(1):16–26.
66. Thiruchelvam U, Wingfield M, O'Farrelly C. Natural Killer Cells: Key Players in Endometriosis. Am J Reprod Immunol. 2015;74(4):291–301.
67. Zhang D, Li Y, Tian J, Zhang H, Wang S. MiR-202 promotes endometriosis by regulating SOX6 expression. Int J Clin Exp Med. 2015;8(10):17757–64.
68. Shen C, Wang B, Zhang K, Wang C, Wang J, An Z, Shu L. RGMB-AS1/miR-4428/PBX1 axis drives the progression of cervical cancer. Transl Cancer Res. 2020;9(5):3180–90.
69. Wu B, Zhang L, Yu Y, Lu T, Zhang Y, Zhu W, Song Q, Lv C, Guo J, Tian Y, et al. miR-6086 inhibits ovarian cancer angiogenesis by downregulating the OC2/VEGFA/EGFL6 axis. Cell Death Dis. 2020;11(5):345.
70. Lee NK, Lee JW, Woo JH, Choi YS, Choi JH. Upregulation of SPI1 in Ectopic Endometrium Contributes to an Invasive Phenotype. Arch Med Res. 2023;54(2):86–94.
71. Yamagata Y, Takaki E, Shinagawa M, Okada M, Jozaki K, Lee L, Sato S, Maekawa R, Taketani T, Asada H, et al. Retinoic acid has the potential to suppress endometriosis development. J Ovarian Res. 2015;8:49.
72. Bigdeli B, Goliaei B, Masoudi-Khoram N, Jooyan N, Nikoofar A, Rouhani M, Haghparast A, Mamashli F. Enterolactone: A novel radiosensitizer for human breast cancer cell lines through impaired DNA repair and increased apoptosis. Toxicol Appl Pharm. 2016;313:180–94.
73. Chen JJ, Xiao ZJ, Meng X, Wang Y, Yu MK, Huang WQ, Sun X, Chen H, Duan YG, Jiang X, et al. MRP4 sustains Wnt/β-catenin signaling for pregnancy, endometriosis and endometrial cancer. Theranostics. 2019;9(17):5049–64.
74. Ivanga M, Labrie Y, Calvo E, Belleau P, Martel C, Luu-The V, Morissette J, Labrie F, Durocher F. Temporal analysis of E2 transcriptional induction of PTP and MKP and downregulation of IGF-I pathway key components in the mouse uterus. Physiol Genomics. 2007;29(1):13–23.
75. Wallis B, Bowman KR, Lu P, Lim CS: The Challenges and Prospects of p53-Based Therapies in Ovarian Cancer. Biomolecules 2023, 13(1).
76. Wang Y, Xue L. Decoding the role of FOXP3 in esophageal cancer: Underlying mechanisms and therapeutic implications. BBA-REV Cancer. 2024;1879(6): 189211.

Publisher's Note